Patterns of skull development in anurans: size and shape relationship during postmetamorphic cranial ontogeny in five species of the Leptodactylus fuscus *Group (Anura: Leptodactylidae)*

María Laura Ponssa & M. Florencia Vera Candioti

Zoomorphology
Evolutionary, Comparative and Functional Morphology

ISSN 0720-213X

Zoomorphology
DOI 10.1007/s00435-012-0164-1

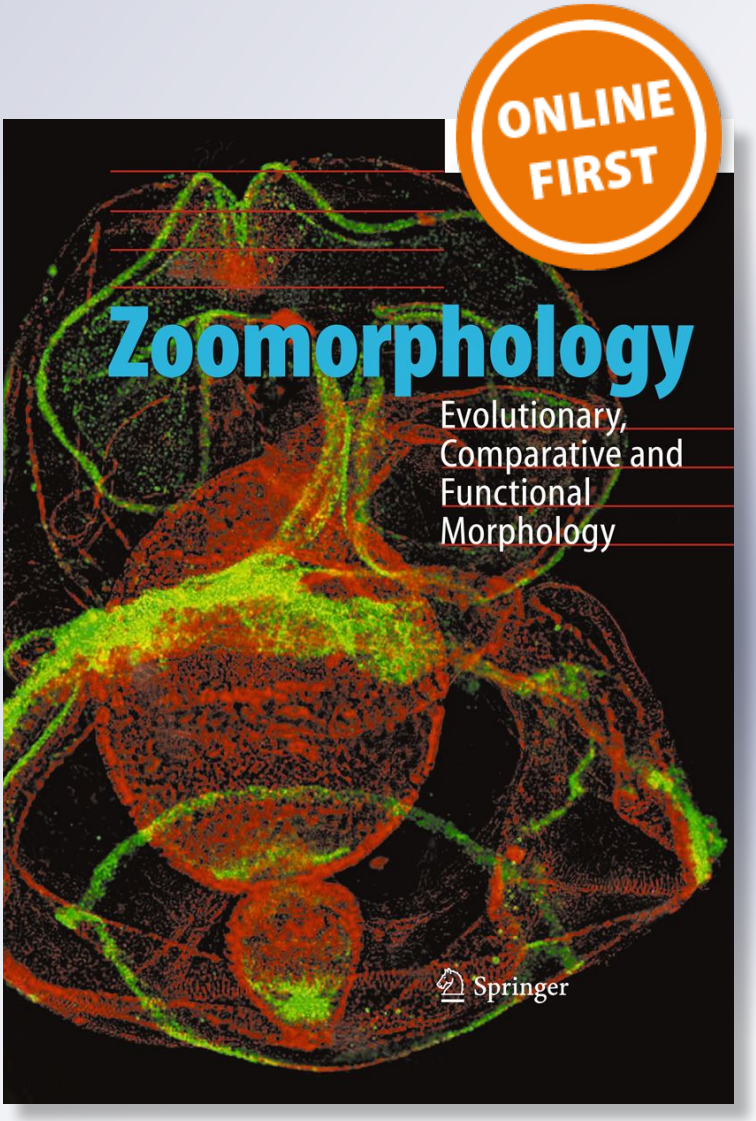

Springer

Zoomorphology
DOI 10.1007/s00435-012-0164-1

ORIGINAL PAPER

Patterns of skull development in anurans: size and shape relationship during postmetamorphic cranial ontogeny in five species of the *Leptodactylus fuscus* Group (Anura: Leptodactylidae)

María Laura Ponssa · M. Florencia Vera Candioti

Received: 26 August 2011 / Revised: 30 May 2012 / Accepted: 5 June 2012

Abstract The effect of allometric ontogenetic changes on morphology has been examined primarily in larval stages of anurans. To our knowledge, such studies after metamorphosis are non-existent, and this information is important because the skull acquires its adult configuration in that period. Using geometric morphometrics, we studied postmetamorphic shape changes in the skull of five species of the *Leptodactylus fuscus* Group (*Leptodactylus bufonius*, *Leptodactylus elenae*, *Leptodactylus fuscus*, *Leptodactylus latinasus*, and *Leptodactylus mystaceus*), a group of small- to medium-sized frogs. Size change is an important factor in explaining shape change during postmetamorphic growth in four of these species; ontogenetic trajectories have in general parallel directions and similar rates of shape change. *L. latinasus* skulls tend to differ in size and shape from the others, and the allometric model, although significant, explains low percentages of shape change. The diverging slope of its ontogenetic trajectory indicates non-heterochronic, allometric repatterning change regarding the ontogenies of *L. bufonius*, *L. elenae*, and *L. fuscus*. Conversely, ontogenetic scaling appears as the main mechanism modeling shape change as regard to *L. mystaceus*; hence, we suggest that a process of progenesis determines the small, juvenile-like cranium of *L. latinasus*. The disparity analysis shows a broader morphological divergence in metamorph morphospace than in adults, suggesting that postmetamorphic stages can contribute with informative characters to phylogenetic analysis. Differences in shapes between metamorphs and adults indicate that many changes occur after metamorphosis, but whether these changes result from internal or ecological requirements at different stages remains unknown.

Keywords Allometry · Geometric morphometrics · Ontogenetic trajectories

Communicated by T. Bartolomaeus.

Electronic supplementary material The online version of this article (doi:10.1007/s00435-012-0164-1) contains supplementary material, which is available to authorized users.

M. L. Ponssa (✉) · M. F. V. Candioti
Instituto de Herpetología, Fundación Miguel Lillo, CONICET, Miguel Lillo 251, San Miguel de Tucumán, Argentina
e-mail: mlponssa@hotmail.com

Introduction

Allometry is the dependence of shape on size, and it is a dominant factor of morphological variation, reflecting the abundant variation of size (Klingenberg 2010). This dependence differs among closely related species; thus, the importance of analyzing the similarity of allometric patterns is that they reflect evolutionary change in growth patterns (Klingenberg 2010). Allometric growth through development can have a profound impact on the shape of morphological structures (Emerson and Bramble 1993; Gould 1966; Larson 2005), and studies of this kind may provide useful data for identifying the developmental roots of functional differences among species and higher taxa (Goswami and Prochel 2007).

Evolution of ontogenetic, allometric trajectories involves three different kinds of changes (revised in Klingenberg 1998): trajectories can change their direction (change in slope), they can shift parallel (lateral transposition), or they can be extended or truncated along the ancestral trajectory (ontogenetic scaling). Diversity in ontogenetic trajectories, besides morphological variation

Published online: 08 July 2012

occurring within and among comparable developmental stages—disparity in morphospace—becomes then the focus of interest to explore in a comparative context of related species. In this sense, allometry offers an operational framework to place disparity in a developmental context (Gerber et al. 2008). The role of the ontogeny in species divergence is little known, but several recent works have begun to explore the variation of phenotypic diversity over development in various zoological groups (e.g., Eble 2003; Zelditch et al. 2003; Gerber et al. 2007; Wilson and Sánchez-Villagra 2010; Frédérich and Vandewalle 2011). The comparison between adults and juveniles combined with statistical analyses of ontogenetic trajectories allows the detection of changes in disparity through ontogeny and the assessing of the role of development in adult disparity (Gerber et al. 2008). Among amphibians, the contribution of ontogenetic allometry to morphological change has been studied primarily in urodeles (Alberch and Alberch 1981; Hanken 1984; Dzukic et al. 1990; Djorović and Kalezić 2000; Ivanović et al. 2007). In anurans, some research has been done on larval stages (Larson 2002, 2004, 2005), but, to our knowledge, studies concerning the contribution of allometry to morphological change in postmetamorphic specimens are non-existent.

The anuran genus *Leptodactylus* (Leptodactylidae) is divided into five species groups (*Leptodactylus ocellatus*, *Leptodactylus melanonotus*, *Leptodactylus pentadactylus*, *Leptodactylus fuscus,* and *Leptodactylus marmoratus* Groups), which represent an evident tendency toward a terrestrial mode of life according to the oviposition mode (Heyer 1969). *Leptodactylus* is an ideal taxon to study the relationship between ontogenetic allometry and shape differences. The genus contains a wide range of different-sized species: it includes large (i.e., *L. pentadactylus* Group) and small (i.e., *L. marmoratus* Group) species. This diversity in size is relevant because it was suggested that in groups in which variation in body size is pronounced, the relationship between morphological parameters and body size can provide valuable information about the developmental base of morphological variation among species (Shea 1983, 1985). In this study, we explore the relationship between size and shape in an assemblage of medium-sized species of the *L. fuscus* Group. This group is the most specious, with 28 species (Frost 2011). The males construct subterranean chambers in which the foam nest with the eggs is placed and the first larval stages develop (Heyer 1969). Three osteological characters (tectum nasi at the same level as the alary process of premaxilla, posterior margin of frontoparietal convex, and cultriform process of parasphenoid between neopalatines) support the monophyly of this group (Ponssa 2008). Members of the group vary widely in size: among the smallest is *L. latinasus* (male snout-vent length − SVL = 31.02 ± 1.7 mm; Heyer 1978), whereas *L. fuscus* is medium-sized (male SVL = 42.8 ± 4.0 mm; Heyer 1978).

In this paper, we apply for the first time a geometric morphometric approach to describe ontogenetic shape changes in the cranial skeleton among *Leptodactylus* and to assess species differences in postmetamorphic ontogenetic allometric trajectories. Specifically, our goals were as follows: (1) to explore the shape changes in the skull of five species of the *L. fuscus* Group, with emphasis on interspecific variation, intraspecific ontogenetic variation, and levels of shape disparity between developmental stages, and (2) to compare ontogenetic trajectories to identify the changes in allometric patterns.

Materials and methods

We studied five species of the *L. fuscus* Group, the phylogenetic relationships (proposed on base of morphological characters in Ponssa et al. 2010) of which are illustrated in Fig. 1. Species examined are *Leptodactylus bufonius* Boulenger, 1894; *Leptodactylus elenae* Heyer 1978; *Leptodactylus fuscus* Schneider, 1799; *Leptodactylus latinasus* Jiménez de la Espada, 1875; and *Leptodactylus mystaceus* Spix, 1824. *L. bufonius* is the most basal in the Group; *L. elenae* and *L. mystaceus* are closely related, belonging to the "*L. mystaceus* species complex" because of their morphological similarities (Heyer et al. 1996); *L. latinasus* and *L. fuscus* are more related to each other than to the other three species, but they belong to two different, less inclusive clades. A total of 99 metamorphic and adult specimens (4–6 metamorphic specimens per species and 8–20 adults per species; Appendix 1, ESM) were processed for qualitative and quantitative analyses of postmetamorphic cranial anatomy. Individuals of some species were collected as larvae and reared until they reached Stage 46 (Gosner 1960), whereas individuals of other species were collected in the field and identified as

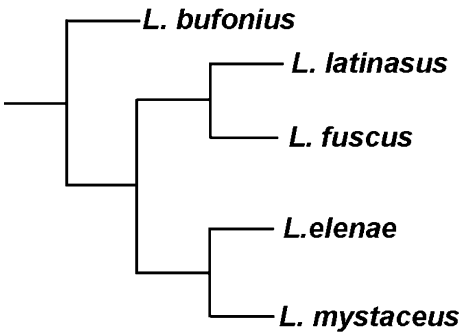

Fig. 1 Abbreviated cladogram showing the phylogenetic relationships of the studied species of the *Leptodactylus fuscus* Group, according to the hypothesis proposed by Ponssa et al. (2010)

Stage 46 metamorphs (and not as more advanced juveniles) based on their size. In other cases, we used specimens deposited in the herpetological collections of the Institute of Herpetology (Fundación Miguel Lillo), Museu de Zoologia Universidade de São Paulo, and National Museum of Natural History (Smithsonian Institution). Assessment of sexual maturity and identification of adult males was based on the presence of secondary sexual characters (i.e., colored vocal sacs); sexual maturity of females was based on examination of the gonads. Specimens were cleared and double-stained for bone and cartilage using the technique of Wassersug (1976). A weak point in our research is the relatively small sample size of metamorphic specimens, which is shown to have different effects on the estimation

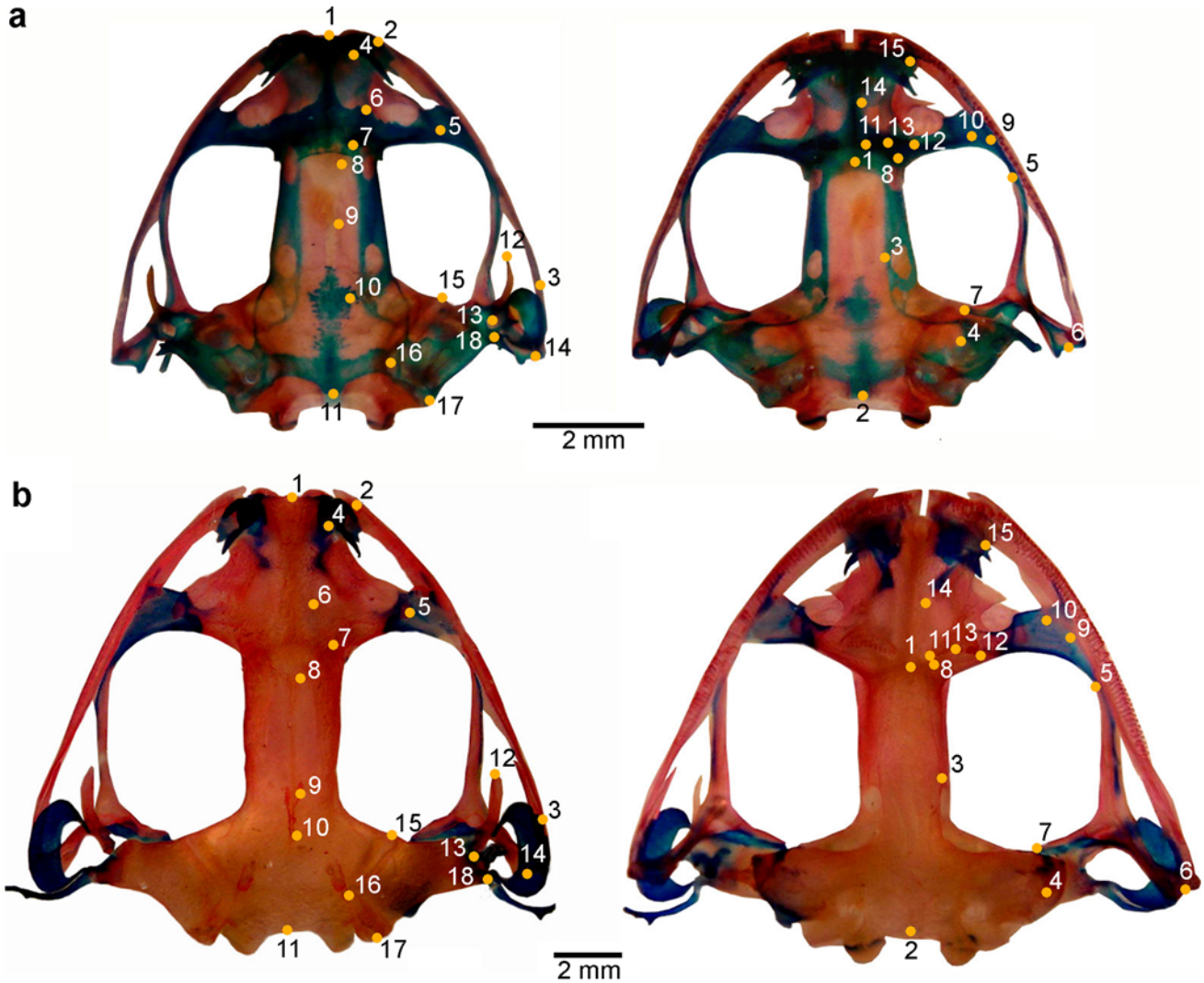

Fig. 2 Landmarks digitized on crania of metamorphs and adults of five species of the *L. fuscus* Group. **a** *L. elenae* metamorph (FML 11916), **b** *L. latinasus* adult (FML 3539). Landmarks in dorsal view (*left*): *1* most anterior point of the tectum nasi, *2* premaxilla–maxilla joint, *3* most posterior point of the maxilla, *4* most anterior point of the nasal, *5* most posterolateral point of the nasal, *6* most medial point of the nasal, *7* most anterior point of the frontoparietal, *8* most anteromedial point of the frontoparietal, *9* most medial point of the frontoparietal, *10* point of the medial margin of the frontoparietal at the level of the most anterior point of the otic capsule, *11* most caudal point of the skull, *12* distal point of the zygomatic ramus of the squamosal, *13* distal point of the otic ramus of the squamosal, *14* distal point of the descendent ramus of the squamosal, *15* most anterior point of the otic capsule, *16* most medial point of the otic capsule, *17* most caudal point of the otic capsule, *18* most lateral point of the otic crista. Landmarks in ventral view (*right*): *1* anterior point of the parasphenoid, *2* most posterior point of the parasphenoid, *3* most lateral point in the margin of the cultriform process of the parasphenoid, *4* most lateral point in the ala of the parasphenoid, *5* distal point of the anterior ramus of the pterygoid, *6* distal point of the posterior ramus of the pterygoid, *7* distal point of the medial ramus of the pterygoid, *8* most medial point of the palatine, *9* most lateral point of the palatine, *10* point of maximum curvature of the anterior margin of the palatine, *11* most medial point of the dentigerous process of the vomer, *12* most lateral point of the dentigerous process of the vomer, *13* middle point of the dentigerous process of the vomer, half-length between landmarks 11 and 12, *14* most medial point of the vomer, *15* distal point of the anterior ramus of the vomer

of several parameters (Cardini and Elton 2007). We tried to moderate this by performing non-parametric, permutation tests whenever possible, but nevertheless, we call the attention on this subject when our conclusions are to be interpreted.

Images of the skulls in dorsal and ventral views were recorded with a Sony Cyber Shot digital camera. We applied geometric morphometric analysis to quantify size-related shape change. The same person (M. L. P.) digitized 18 dorsal and 15 ventral landmarks with TpsDig ver. 2.16 software (Rohlf 2010a) on the right half of each skull image (Fig. 2; landmarks defined in caption). We selected the landmarks based on their ease of identification in all specimens and their capacity to represent the entire geometric form and to provide functional descriptions of important regions of the skull (Larson 2002).

Standard geometric morphometric analyses were done with TPS and MorphoJ software (Rohlf 2010b; Klingenberg 2011). Landmark configurations for each specimen were translated, standardized to centroid size = 1, and aligned through the generalized Procrustes analysis (GPA) to produce a consensus configuration, and we obtained partial warp and uniform component scores (Rohlf and Bookstein 1990; Bookstein 1991; Zelditch et al. 2004). The data set was first analyzed with a canonical variate analysis (CVA) on shape coordinates; this method maximizes the differences between groups relative to the variation within groups and is therefore the most efficient method for detecting separation among developmental stages and species (Klingenberg et al. 2011). The statistical significance of pairwise differences in mean shapes of the ten groups (2 stages × 5 species) was assessed with permutation tests using Procrustes distance as the test statistic (10,000 permutations per test). Holm's sequential Bonferroni correction was applied to adjust p values in multiple comparisons (Holm 1979).

Size information was saved to analyze differences among metamorph and adult crania; an ANOVA on centroid size (CS) was first performed. To analyze ontogenetic, size-related shape change, we used multivariate regression of shape (the Procrustes coordinates) on log-transformed CS separately for each species (Drake and Klingenberg 2008). The null hypothesis being tested states that shape develops isometrically; thus, a significant result points out that shape changes according to a predictable model with increasing size. The amount of variation for which the regression model accounted was quantified as a percentage of the total shape variation, computed using the Procrustes metric (Klingenberg and McIntyre 1998). The statistical significance of the regressions was tested with permutation tests against the null hypothesis of independence (Drake and Klingenberg 2008). To look for differences in allometric trajectories among species, we carried out a MANCOVA (homogeneity of slopes test), with the Procrustes coordinates as dependent variables, logCS as covariate, and species as grouping factor. When slopes did not differ, the MANCOVA was repeated after removing the interaction term, and differences in regression intercepts were tested; this indicates whether allometric trajectories are similar (parallel or laterally transposed) or the same (Viscosi and Cardini 2011). When slopes differed, two possibilities were explored further. First, we calculated the angle between multivariate regression vectors of pairs of species (Veccompare6, IMP software; Sheets 2004; Zelditch et al. 2004). The statistical significance of the angles calculated was tested using a bootstrap procedure. If the between-species angle is larger than the 95 % range of the bootstrapped within-species angles, the between-species angle is considered significantly different from 0°, and allometric trajectories are different. Second, to determine whether species differ in the rate of development along the same ontogenetic trajectory, we regressed the Procrustes distance between each specimen and the average metamorph on lnCS (Regress6; IMP software; Sheets 2004; Zelditch et al. 2004). To compare developmental rates among species, we used ANCOVA with Procrustes distances as the dependent variable, lnCS as the covariate, and species as the grouping factor. Significant differences in developmental rate were inferred from a statistically significant species × lnCS interaction (Zelditch et al. 2004).

Finally, morphological disparity in cranial shapes of metamorphs (measured at the average centroid size) and adults (measured at maximum centroid size) of the five *Leptodactylus* species was calculated following the method described in Zelditch et al. (2000) and (2004), which provides an estimate of species dispersion around a grand mean shape, with confidence intervals and standard errors obtained by a bootstrap procedure. The partial disparity of each taxon represents its contribution to the overall disparity around the mean shape. The level of metamorph disparity is then compared to that of adults in order to describe the dynamics of shape disparity through ontogeny. All calculations were done with DisparityBox6 (IMP software; Sheets 2004; Zelditch et al. 2004).

Results

Skull size

Skull length measurements (from the anterior most point of the premaxilla to the occipital condyle) are as follows: *L. bufonius*: metamorphs: 4.61 mm (4.1–5.33)/adults: 17.22 (14.66–19.53); *L. elenae*: 10.64 mm (10.2–11.85)/16.17 (14.87–18.88); *L. fuscus*: 8.6 mm (7.89–10.98)/16.19 (14.56–18.56); *L. latinasus*: 7.01 mm (4.05–8.73)/10.97 (9.19–13.27);

Table 1 ANOVA of centroid size (skull dorsal view) of metamorph and adult crania of five species of the *L. fuscus* Group; Bonferroni post hoc test results

		b	e	f	l	m	b	e	f	l
Metamorph	e	*								
	f	*	0.22							
	l	1	*	0.34						
	m	1	*	1	1					
Adult	b	*	*	*	*	*				
	e	*	*	*	*	*	*			
	f	*	*	*	*	*	0.32	1		
	l	*	1	*	*	*	*	*	*	
	m	*	*	*	*	*	1	0.03	1	*

Metamorph Adult

Cells in *light gray* show metamorph–metamorph comparisons, cells in *medium gray*, metamorph–adult comparisons, and cells in *dark gray*, adult–adult comparisons. *p* values indicating significant differences are represented by *asterisks* (*p* values adjusted after sequential Bonferroni correction). *b, L. bufonius*; *e, L. elenae*; *f, L. fuscus*; *l, L. latinasus*; *m, L. mystaceus*

L. mystaceus: 7.1 mm (6.19–8.71)/17.10 (15.62–19.18). The results of ANOVA on centroid size of metamorph and adult crania measured from the landmark configuration in dorsal view are shown in Table 1 ($F = 120.93$, $p < 0.005$; results for ventral view are almost identical and thus not shown). The Bonferroni post hoc tests show most adults (dark gray cells) to resemble one another, excepting *L. bufonius* from *L. elenae* (not different with ventral data: $p = 0.33$), and *L. latinasus*, which are smaller than the remaining species. Metamorphs (light gray cells) are similar in size, excepting *L. fuscus* from *L. bufonius*, and *L. elenae*, which are larger than *L. bufonius, L. latinasus*, and *L. mystaceus*. Pairwise comparisons between metamorphs and adults of all species (medium gray cells) result in significant differences, except for adult *L. latinasus*, which resemble the metamorphs of *L. elenae*.

Skull shape

The CVA of the dorsal skull data set ($n = 99$) is shown in the scatter plot of the first and second canonical variates (CV1 vs. CV2; Fig. 3 left). CV1 captures 56.2 % of the total skull shape variation and together with CV2 accounts for 72.90 % of the variation; the remaining percentages are listed in Appendix 2, ESM. CV1 recovers ontogenetic shape change, with variation concentrated in the enlargement of the mandible (landmarks 2–3), the nasals (landmarks 4–6), and the squamosal, which also changes its vertical position to a more horizontal one (landmarks 12–14). Differences among species are outlined on CV2, with a shorter mandible in species with lower scores (e.g., metamorphs of *L. elenae* and *L. latinasus*). In CVA of the ventral skull ($n = 94$; Fig. 3 right; Appendix 3, ESM), CV1 explains 72.97 % of the total shape variation and together with CV2 accounts for 83.76 % of the variation. The deformation grids along the CV1 describe shape change associated with a widening of the pterygoid caused by the increased separation between the medial and posterior rami; furthermore, the pterygoid rotates to a more vertical position (landmarks 5–7). There is also a widening of the caudal region of the parasphenoid (landmarks 2 and 4), a curvature of the dentigerous process of the vomer (landmarks 11–13), and an enlargement of the neopalatine (landmarks 8–10). On CV2, shape change is concentrated in the enlargement of the neopalatine.

Procrustes distances among groups are listed in Table 2. In dorsal view, *p* values show that all adults (dark gray cells) are different from each other and regarding metamorphs (medium gray cells); all metamorphs (light gray cells) differ in shape, excepting *L. latinasus* and *L. mystaceus.* Likewise, in skull ventral view, all adults are different from each other and regarding metamorphs; in metamorph–metamorph morphospace, *L. latinasus* resembles *L. elenae*, *L. fuscus*, and *L. mystaceus*, and *L. fuscus* is similar to *L. mystaceus.*

Ontogenetic trajectories

Based on landmark configurations of dorsal and ventral views of the skulls, we reject the null hypothesis of isometric growth in all five species, because the regressions accounted for statistically significant ($p < 0.001$), high percentages of the shape variation in all cases (% of shape variation explained by size in dorsal/ventral skull:

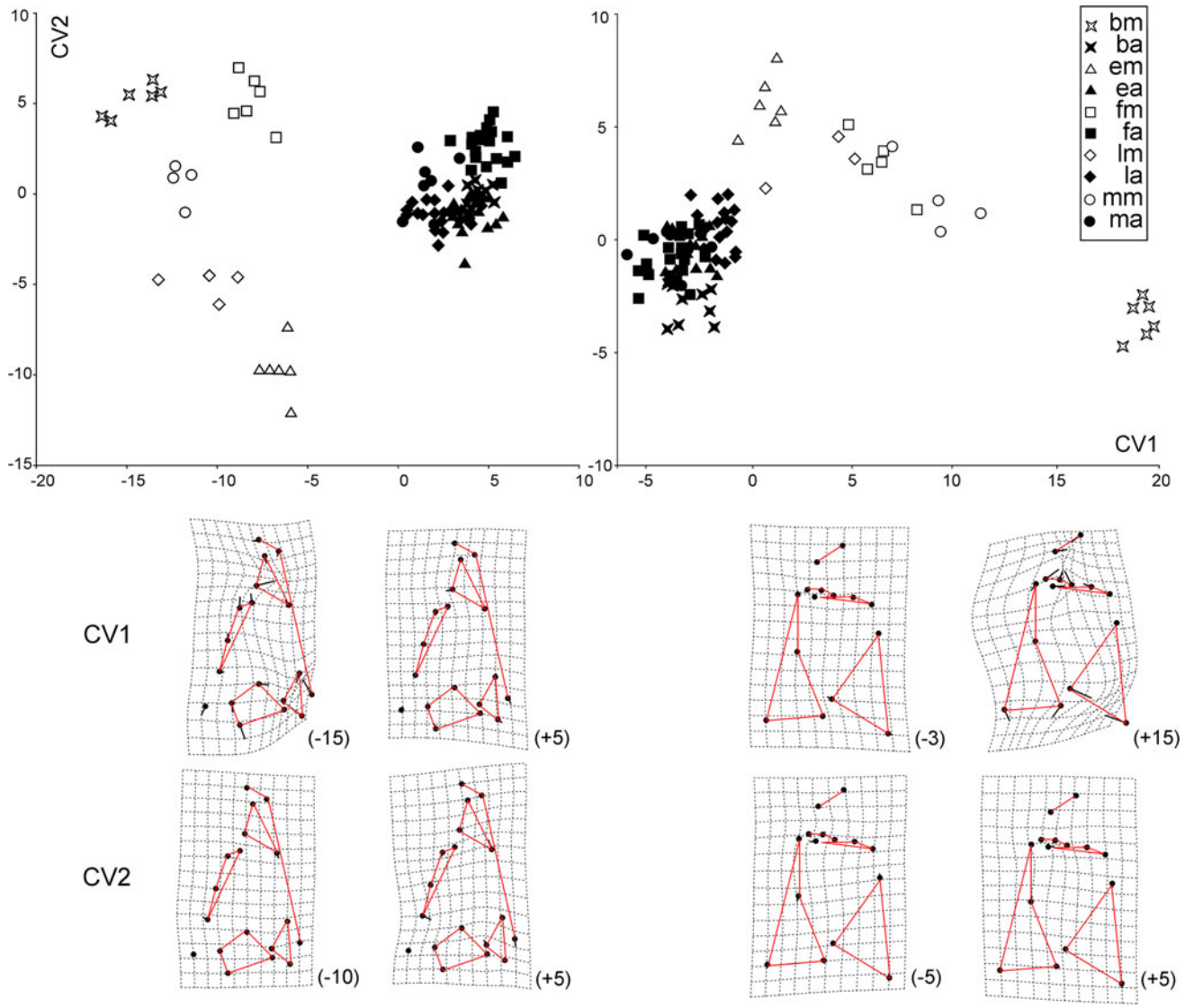

Fig. 3 CVA on shape coordinates of skull configuration in dorsal (*left*) and ventral (*right*) views, in five species of the *L. fuscus* Group. The deformation grids show the shape variation along each axis regarding the consensus (average) configuration; the numbers between parentheses are the scores each grid corresponds. In dorsal view, CV1 recovers ontogenetic shape change, with variation concentrated in the enlargement of the mandible (landmarks 2–3), the nasals (landmarks 4–6), and the squamosal, which also changes its vertical position to a more horizontal one (landmarks 12–14). The CV2 outlines interspecific differences, with a longer mandible in species with higher scores. In ventral view, shape change in CV1 is associated with a widening of the pterygoid, which also adopts a more vertical position (landmarks 5–7), widening of the caudal region of the parasphenoid (landmarks 2 and 4), curvature of the dentigerous process of the vomer (landmarks 11–13), and an enlargement of the palatine (landmarks 8–10). On CV2, shape change is concentrated in the enlargement of the palatine. *ba, L. bufonius* adult; *bm, L. bufonius* metamorph; *ea, L. elenae* adult; *em, L. elenae* metamorph; *fa, L. fuscus* adult; *fm, L. fuscus* metamorph; *la, L. latinasus* adult; *lm, L. latinasus* metamorph; *ma, L. mystaceus* adult; *mm, L. mystaceus* metamorph

L. bufonius: 69.88/74.55; *L. elenae*: 50.35/32.29; *L. fuscus*: 45.34/43.56; *L. latinasus*: 52.07/17.14; *L. mystaceus*: 67.07/61.59) (Figs. 4, 5). The MANCOVA results show significant differences in at least one pair of ontogenetic trajectory slopes, both from dorsal and ventral landmark configurations (dorsal: Wilks' Lambda = 0.004, $p < 0.001$; ventral: Wilks' Lambda = 0.029, $p < 0.001$). Species–species comparisons (Table 3) show that in dorsal skull, the ontogenetic trajectory of *L. latinasus* differs from those of *L. bufonius*, *L. elenae*, and *L. fuscus* ($p < 0.01$), and *L. fuscus* differs from *L. elenae* ($p = 0.00004$). In ventral skull, *L. bufonius* differs from *L. elenae*, *L. fuscus*, and *L. mystaceus* ($p < 0.01$), and *L. fuscus* differs from *L. elenae* ($p = 0.00004$). In the remaining pairwise comparisons

Table 2 Procrustes distances among groups (species × developmental stages), in five species of the *L. fuscus* Group; Bonferroni post hoc test results

			Metamorph					Adult				
			b	e	f	l	m	b	e	f	l	m
DORSAL	Metamorph	b		*	*	*	*	*	*	*	*	*
		e	0.1369		*	*	*	*	*	*	*	*
		f	0.0880	0.0945		*	*	*	*	*	*	*
		l	0.0884	0.1004	0.0839		0.29	*	*	*	*	*
		m	0.1016	0.1141	0.0792	0.0654		*	*	*	*	*
	Adult	b	0.1886	0.1385	0.1616	0.1827	0.2131		*	*	*	*
		e	0.1683	0.0995	0.1314	0.1532	0.1781	0.0670		*	*	*
		f	0.1680	0.1153	0.1301	0.1572	0.1833	0.0636	0.0498		*	*
		l	0.1717	0.1042	0.1425	0.1558	0.1846	0.0683	0.0449	0.0587		*
		m	0.1610	0.1025	0.1260	0.1539	0.1785	0.0568	0.0321	0.0367	0.0526	
VENTRAL	Metamorph	b		*	*	*	*	*	*	*	*	*
		e	0.1948		*	0.02	*	*	*	*	*	*
		f	0.1526	0.0611		0.06	0.03	*	*	*	*	*
		l	0.1746	0.0704	0.0652		0.05	*	*	*	*	*
		m	0.1151	0.1143	0.0769	0.0952		*	*	*	*	*
	Adult	b	0.2172	0.1064	0.1194	0.1028	0.1454		*	*	*	*
		e	0.2241	0.0917	0.1100	0.0922	0.1446	0.0489		*	*	*
		f	0.2310	0.0949	0.1132	0.1000	0.1427	0.0555	0.0383		*	*
		l	0.1983	0.0876	0.0929	0.0763	0.1167	0.0548	0.0507	0.0523		*
		m	0.2311	0.0801	0.1113	0.0992	0.1492	0.0511	0.0415	0.0417	0.0574	

Values below each main diagonal are Procrustes distances, and cells above it contain *p* values (adjusted after sequential Bonferroni correction). Cells in *light gray* show metamorph–metamorph comparisons, cells in *medium gray*, metamorph–adult comparisons, and cells in *dark gray*, adult–adult comparisons. *p* values indicating significant differences are represented by *asterisks*. *b, L. bufonius*; *e, L. elenae*; *f, L. fuscus*; *l, L. latinasus*; *m, L. mystaceus*

with non-significantly different slopes, intercepts are different between the trajectories of *L. bufonius–L. elenae* and *L. bufonius–L. fuscus* (dorsal skull; $p < 0.001$), and between *L. elenae–L. mystaceus* and *L. latinasus* and all the remaining species (ventral skull; $p < 0.05$).

Angles of allometric vectors (Table 4) differ significantly from 0° in all comparisons but *L. latinasus–L. bufonius* (dorsal skull), and *L. bufonius–L. fuscus* and *L. bufonius–L. mystaceus* (ventral skull). Rates of increase in the Procrustes distance (from metamorph to adult shape) relative to size are not significantly different (dorsal skull: ANCOVA $F = 1.0291$, $p = 0.39$; ventral skull: ANCOVA $F = 0.8353$, $p = 0.50$). Developmental rates in all species are compared in Table 5, in which the overlapping dispersion measurements are listed.

Morphological disparity

Cranial shape disparity decreases during ontogeny, both in dorsal and ventral configurations. In dorsal skull view, metamorphs are 3 times more disparate than adults, and *L. elenae* has the largest partial disparity percentage among them, whereas *L. bufonius*, *L. fuscus*, and *L. latinasus* contribute with high and similar percentages to the overall adult disparity (Table 6, top). In ventral skull, metamorph disparity is twice larger than that of adults, and *L. bufonius* and *L. fuscus* are the more disparate of metamorphs and adults, respectively (Table 6, bottom). Patterns of shape variation are depicted in Fig. 6, showing the broader shape diversity in metamorph geometry.

Table 3 Results of MANCOVA tests of homogeneity of slopes and intercept differences, in ten pairwise comparisons of skull shape in five species of the *L. fuscus* Group

Sp1	Sp2	Slopes		Intercept	
		Wilks' Lambda	*p*	Wilks' Lambda	*p*
Dorsal					
b	e	0.0140	0.07	0.0052	0.003*
	f	0.0889	0.13	0.0317	0.002*
	l	0.0088	0.009*		
	m	0.0034	0.22	0.0011	0.13
e	f	0.0398	0.00004*		
	l	0.0711	0.01*		
	m	0.0048	0.29	0.0006	0.11
f	l	0.0963	0.003*		
	m	0.0572	0.40	0.0520	0.22
l	m	0.0017	0.18	0.0045	0.29
Ventral					
b	e	0.0200	0.0008*		
	f	0.0469	0.0003*		
	l	0.0781	0.05	0.0234	0.0004*
	m	0.0001	0.01*		
e	f	0.0815	0.00004*		
	l	0.3125	0.44	0.1187	0.004*
	m	0.0379	0.09	0.0400	0.04*
f	l	0.3079	0.20	0.1364	0.001*
	m	0.1083	0.08	0.2564	0.53
l	m	0.0619	0.21	0.0169	0.006*

Significantly different values ($p < 0.05$) are followed by an asterisk

Discussion

Within the species studied, *L. bufonius, L. elenae, L. fuscus,* and *L. mystaceus* have several common cranial features and development. Skull size is similar among all adults and among metamorphs (excepting those of *L. elenae,* which are larger), and skull shape allows to distinguish most species from each other. As shown by allometric models, size change is an important factor in explaining shape change during postmetamorphic growth in these species. Also, ontogenetic trajectories have in general parallel directions and similar rates of shape change. In several species–species comparisons (e.g., *L. bufonius* regarding *L. fuscus* and *L. elenae*, and *L. latinasus* regarding the remaining four species; Table 3) a lateral transposition is inferred from differences in the regression intercepts, and in terms of shape variation, this means that even when the shape of the skulls may differ, the trend of covariation with size is similar (Viscosi and Cardini 2011). In those cases where the intercepts of the trajectories are not significantly different (e.g., *L. mystaceus* regarding the four remaining species), the evolutionary change can be interpreted as ontogenetic scaling, pointing out that allometric trajectories overlap among species, and therefore, patterns are the same (Viscosi and Cardini 2011).

Most of the analyses reveal *L. latinasus* to be different from the other four taxa. First, the size analysis shows that adult *L. latinasus* are smaller than adults of the other species, resembling the size of metamorphic *L. elenae*. Likewise, the ventral skull shape in adults tends to diverge and resemble that of the other species metamorphs. Regarding ontogenetic trajectory, although a significant allometric model is found, the percentages of shape change explained by size are among the lowest (especially in the ventral skull configuration). The slope of the ontogenetic trajectory of the dorsal skull diverges from those of *L. bufonius*, *L. elenae*, and *L. fuscus* (with angles significantly different from 0° regarding the two latter; Tables 1, 2), and evolutionary change can be ascribed to allometric repatterning. Conversely, the ontogenetic trajectory shares slope and intercept with that of *L. mystaceus*, and ontogenetic scaling is then postulated as the main mechanism modeling shape change between these two species.

When the trajectories of shape change are conserved between ancestors and descendants, and size is regarded as a proxy for time, the parallelism between ontogeny and phylogeny is retained and Gould's (1977) definition of heterochrony can be applied (Mitteroecker et al. 2005; Webster and Zelditch 2005). Morphological patterns of paedomorphosis (i.e., the retention of ancestral juvenile

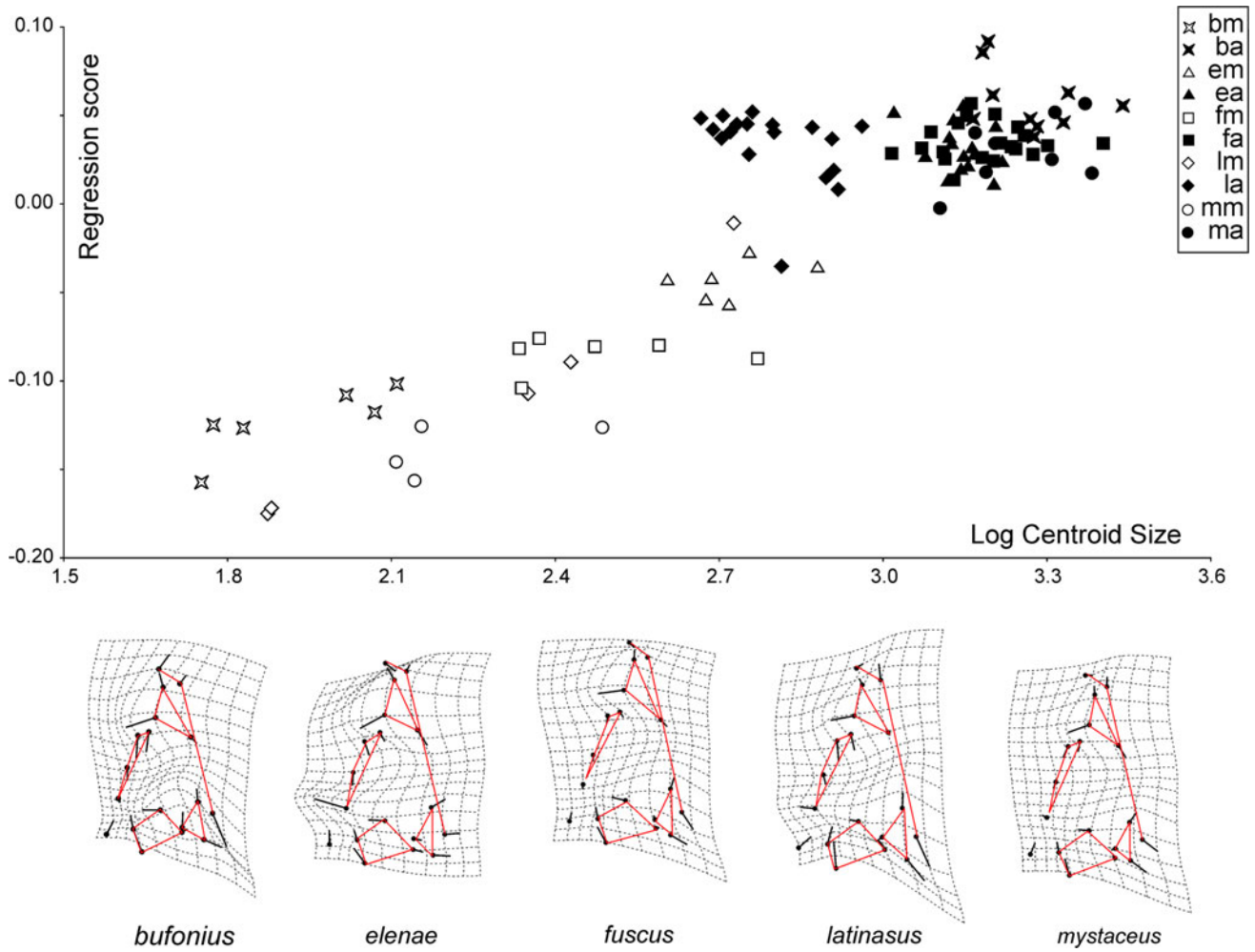

Fig. 4 Allometry of the skull in dorsal view, in five species of the *L. fuscus* Group. The deformation grids show the predicted ontogenetic shape change, as indicated by an increase in log-transformed centroid size by 1 unit in all species excepting *L. bufonius* (2 units). Note the diverging ontogenetic trajectory in *L. latinasus* regarding the remaining species. *ba, L. bufonius* adult; *bm, L. bufonius* metamorph; *ea, L. elenae* adult; *em, L. elenae* metamorph; *fa, L. fuscus* adult; *fm, L. fuscus* metamorph; *la, L. latinasus* adult; *lm, L. latinasus* metamorph; *ma, L. mystaceus* adult; *mm, L. mystaceus* metamorph

characters in the descendent adult phase) and peramorphosis (i.e., the exaggeration of adult traits) can be then revealed. Ontogenetic scaling, when it is found without other changes to growth trajectories, can establish these patterns directly and unambiguously (Klingenberg 1998). Some skull shape features and development in *L. latinasus* point out a paedomorphic pattern regarding *L. mystaceus*. Besides the multivariate allometric effect involving the whole ventral skull that we found in our results (as indicated by adult *L. latinasus* getting closer to metamorph morphospace; Fig. 6), individual osteological characters have been previously proposed to be paedomorphic in *L. latinasus* (Ponssa 2008). Particularly, the dentigerous process of the vomer in adults is straighter than those of the adults of the other species and resembles the dentigerous processes of their metamorphs (Fig. 5). Paedomorphosis can be achieved in three ways: (1) a decrease in the rate at which the trajectory of shape change is followed (alternatively termed as neoteny or deceleration); (2) the late commencement of the trajectory of shape change (post-displacement); and (3) early termination of the trajectory of shape change (alternatively termed as progenesis or hypomorphosis) (Alberch et al. 1979; Fink 1982, 1988; Gould 1977; McNamara 1986; Reilly et al. 1997; Shea 1983). Our results explicitly eliminate the first possibility because the rates of shape change are not significantly different between *L. latinasus* and *L. mystaceus*. On the other hand, adults of *L. latinasus* are significantly smaller than adults of the other species, and this suggests that size (and with it, shape) changes have been stopped precociously. Thus, we

Table 4 Angles between ontogenetic trajectories of species of the *L. fuscus* Group having different ontogenetic trajectories, as indicated by MANCOVA common slopes test, from both dorsal and ventral skull configurations

Sp1	Sp2	Between	Within Sp1	Within Sp2
Dorsal				
f	e	43.8*	24.9	23.8
	l	35.0*	26.0	23.5
l	e	51.3*	23.9	22.9
	b	32.0	33.3	18.8
Ventral				
f	b	33.6	34.1	17.2
	e	40.5*	27.7	31.5
b	e	60.0*	17.9	35.7
	m	25.8	18.7	27.3

Differences between species angles are considered significant (*) when the between-species angle is larger than both the within-species angles, after a bootstrap procedure ($n = 900$). *b, L. bufonius*; *e, L. elenae*; *f, L. fuscus*; *l, L. latinasus*

Table 5 The rates of ontogenetic shape changes (from metamorph to adult shape) and the distance traveled over the unit of the independent variable (lnCS). *b, L. bufonius*; *e, L. elenae*; *f, L. fuscus*; *l, L. latinasus*

	R^2	Slope	SE	Distance traveled (mean)	Distance traveled (range)
Dorsal					
b	0.952363	0.098447	0.008425	0.1470	0.0439–0.2338
e	0.925989	0.1382	0.0126	0.0898	0.0384–0.1317
f	0.8803	0.1119	0.0123	0.1197	0.0377–0.1611
l	0.7350	0.1201	0.0242	0.1722	0.0737–0.2139
m	0.933292	0.122062	0.014853	0.1446	0.0431–0.2285
Ventral					
b	0.987733	0.113946	0.004996	0.1641	0.0524–0.2490
e	0.820216	0.097014	0.015523	0.0887	0.0354–0.1283
f	0.565599	0.135912	0.041321	0.1373	0.0503–0.3880
l	0.755838	0.081122	0.016122	0.0888	0.0396–0.1211
m	0.954758	0.085677	0.008439	0.1308	0.0639–0.1926

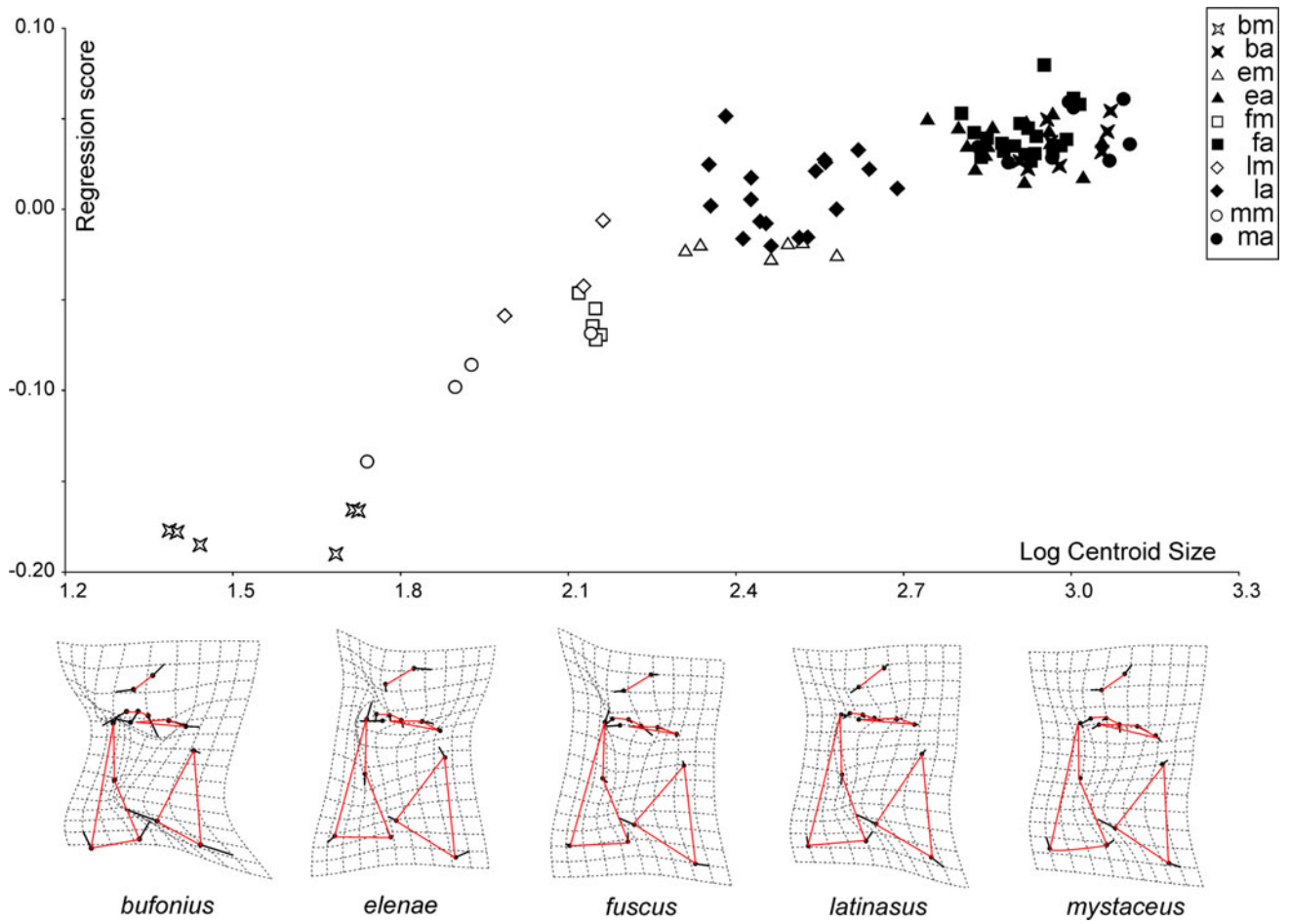

Fig. 5 Allometry of the skull in ventral view, in five species of the *L. fuscus* Group. The deformation grids show the predicted ontogenetic shape change, as indicated by an increase in log-transformed centroid size by 1 unit in all species excepting *L. bufonius* (2 units). Note the dentigerous process of the vomer (landmarks 11–13), straighter in *L. latinasus* grid as compared to the remaining species. *ba, L. bufonius* adult; *bm, L. bufonius* metamorph; *ea, L. elenae* adult; *em, L. elenae* metamorph; *fa, L. fuscus* adult; *fm, L. fuscus* metamorph; *la, L. latinasus* adult; *lm, L. latinasus* metamorph; *ma, L. mystaceus* adult; *mm, L. mystaceus* metamorph

Table 6 Shape disparities (overall and partial, MD and PD), 95 % confidence intervals, and standard errors obtained after bootstrapping, measured in metamorphs and adults of five species of the *L. fuscus* Group in both dorsal and ventral skull configurations. *b, L. bufonius*; *e, L. elenae*; *f, L. fuscus*; *l, L. latinasus*; *m, L. mystaceus*

		PD	SE	%MD
Dorsal				
Metamorph				
MD = 0.0051	b	0.00130	0.00048	25
CI = 0.0050–0.0062	e	0.00176	0.00049	35
SE = 0.003	f	0.00061	0.00053	12
	l	0.00073	0.00044	14
	m	0.00072	0.00044	14
Adult				
MD = 0.0017	b	0.00040	0.00040	24
CI = 0.0019–0.0037	e	0.00020	0.00036	12
SE = 0.0005	f	0.00042	0.00020	25
	l	0.00041	0.00023	24
	m	0.00028	0.00018	16
Ventral				
Metamorph				
MD = 0.0076	b	0.00385	0.00160	54
CI = 0.0073–0.0096	e	0.00173	0.00134	20
SE = 0.0006	f	0.00051	0.00128	6
	l	0.00058	0.00143	13
	m	0.00047	0.00147	7
Adult				
MD = 0.0031	b	0.00058	0.00015	19
CI = 0.0024–0.0068	e	0.00026	0.00083	8
SE = 0.0011	f	0.00099	0.00017	32
	l	0.0006	0.00028	19
	m	0.00061	0.00033	20

propose that a modification in the offset of the ontogenetic trajectory (progenesis) results in the smaller, juvenile-like cranium of *L. latinasus*.

Many authors have focused on shape changes associated with evolution of body size (Hone et al. 2008; Frédérich and Sheets 2010), and particularly on the apparent significance of phylogenetic decrease in size to macro-evolutionary trends and the appearance of morphological novelties (Stanley 1973; Hanken 1984; Wake 1986). The evolution of extremely small body size within a lineage is known as miniaturization—a phylogenetic inference that a lineage evolved from a larger ancestor (Hanken and Wake 1993). Miniaturization frequently is achieved via the precocious truncation of development (Hanken 1984), which also produces a paedomorphic morphology (Yeh 2002). The size of the small adults of *L. latinasus* represents about 60 % of the size of the most basal species in the *L. fuscus* Group (Ponssa 2008) (e.g., *L. labrosus* SVL (males/females) = 54.6 ± 5.3/53.3 ± 6.3 mm; *L. ventrimaculatus* = 50.4 ± 3.5/51.9 ± 4.8 mm; Heyer 1978), and about 22 % of the size of species of the sister clade *L. pentadactylus* Group (e.g., *L. pentadactylus* = 140.8 ± 94.8/154.5 ± 39.2 mm; Heyer 2005). These sizes would not represent cases of miniaturized frogs, because Clarke (1996) and Yeh (2002) considered maximum adult snout-vent lengths of 20 and 25 mm, respectively, to be miniaturized. Nevertheless, we emphasize the significant reduction in size in *L. latinasus*, which is not associated with the loss of skull bones as it is in other taxa, but which could be associated with truncation of development and morphological novelty (Yeh 2002). Along with *L. latinasus*, *L. fragilis,* and *L. caatingae* are the smallest species of the *L. fuscus* Group, and they also share some apparently paedomorphic cranial features (Heyer and Juncá 2003; Ponssa 2008); we hypothesize that similar allometric changes could be modeling cranial shape in these two related small species as well.

Anuran larvae vary much more in the extent of ossification and in morphometric features than do juveniles, because the shapes of most cranial bones are largely determined in juveniles (Djorović and Kalezić 2000). However, differences in shapes between metamorphs and adults indicate that substantial changes occur after metamorphosis. The main changes in shape through postmetamorphic growth occur in the nasal region (enlargement of nasals and vomers) and the posterior area of the skull, with the widening of the otic region and the growth and rotation to a more horizontal position of the squamosals and pterygoids. Substantial changes must occur after metamorphosis to acquire the adult cranium shape, because the metamorph skull is a cartilaginous scaffold, whereas the adult skull emerges from ossification of the scaffold and its overlying investing bones.

Apart from the ontogeny-associated shape change species tend to segregate in both metamorph and adult morphospaces, indicating that there are features inherent to the species that maintain interspecific differences throughout development. Levels of morphological disparity in metamorphs exceed those calculated for adults. However, the observed disparity in metamorphs could be largely biased by differences in the postmetamorphic stages analyzed (e.g., the case of larger metamorphs of *L. elenae*); also, our sample size in metamorphs is relatively small, and as shown by Cardini and Elton (2007), the estimation of mean shapes is strongly affected by sampling error, which can have profound consequences on studies of among-species disparity. In our (thus tentative) results, the metamorphs diverging wider in morphospace than adults could indicate that in some cases it can be easier to discriminate among closely related species of *Leptodactylus* at early stages of postmetamorphosis than older individuals (note also the

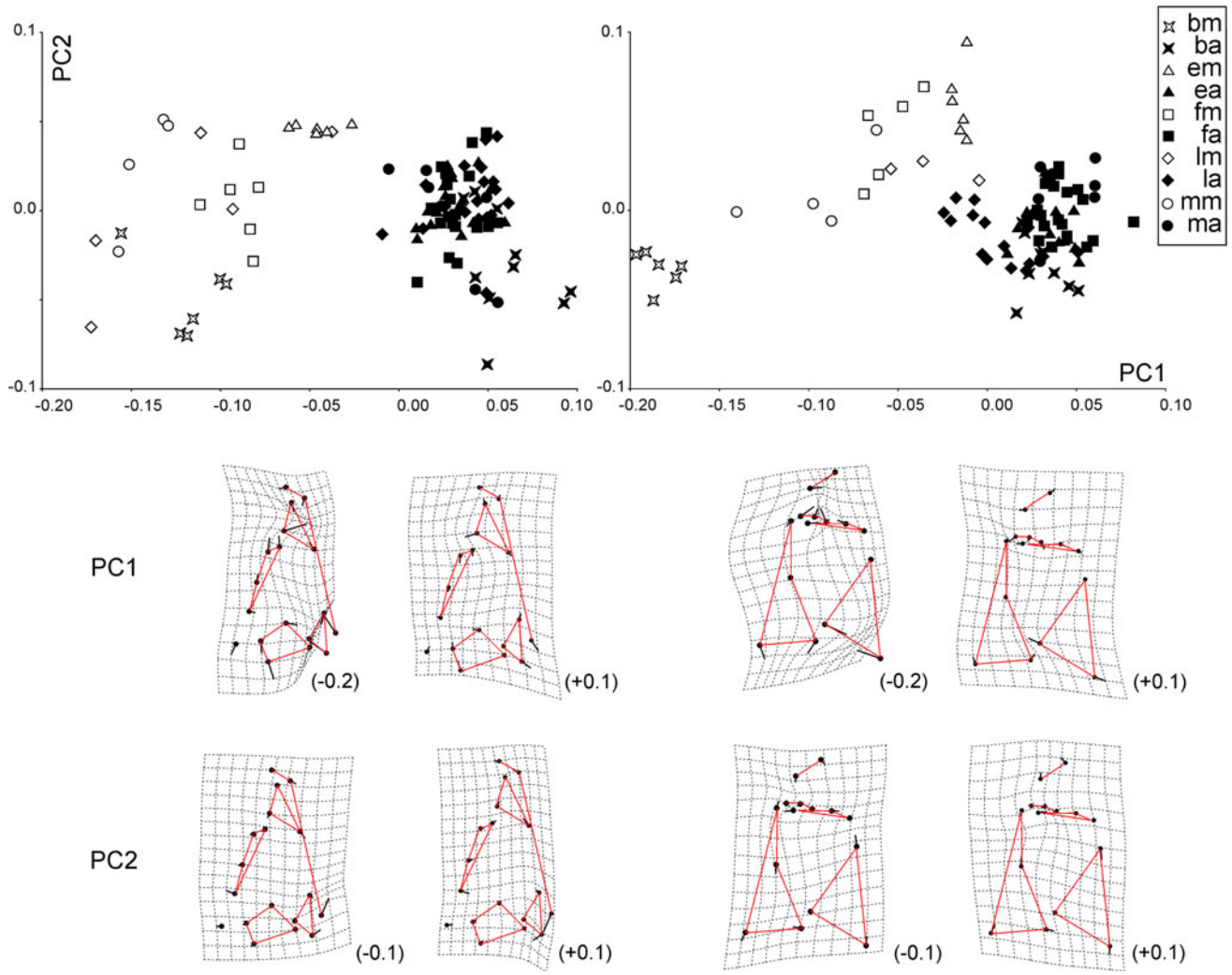

Fig. 6 PCA on shape coordinates of skull configuration in dorsal (*left*) and ventral (*right*) views, in five species of the *L. fuscus* Group, showing the main patterns of variation in shape space. The deformation grids show the shape variation along each axis (highest and lowest scores) regarding to the consensus configuration; the numbers between parentheses are the scores each grid corresponds. Note that shape disparity in metamorphs exceeds that of adults. *ba, L. bufonius* adult; *bm, L. bufonius* metamorph; *ea, L. elenae* adult; *em, L. elenae* metamorph; *fa, L. fuscus* adult; *fm, L. fuscus* metamorph; *la, L. latinasus* adult; *lm, L. latinasus* metamorph; *ma, L. mystaceus* adult; *mm, L. mystaceus* metamorph

Procrustes distances among metamorphs as compared to those among adults in Table 2). Thus, ontogenetic pattern and interspecific variation are directly associated, and allometry would have had a deep impact on the skull shape through the juvenile development in these species. The pattern displayed by the metamorphs does not coincide with the available phylogenetic data with respect to species relationships, and this indicates that additional, taxonomically useful information is available in this semaphoront (i.e., juvenile) stage. In an attempt to explain ontogenetic patterns of shape disparity, Ciampaglio (2002) summarizes two categories of factors: the external (ecological) constraints and the internal (developmental, genetic, or functional) constraints. In agreement with our results, studies by Zelditch et al. (2003) and Adams and Nistri (2010) on other ectotermic vertebrates found that the disparity decreases significantly over ontogeny, in piranhas and European cave salamanders, respectively. Whereas in the case of piranhas, the pattern is explained in terms of developmental constrains (Zelditch et al. 2003), Adams and Nistri (2010) interpret the lower disparity of adult salamanders as a consequence of a morphology more functionally constrained than that of juveniles. In our case, we lack ecological data as to either support or discard a functional explanation for the observed pattern of ontogenetic disparity. We found allometric, ontogenetic

differences in feeding structures (e.g., mandible and squamosal), which serve as point of attachment for adductor muscles involved in the jaw closing (Duellman and Trueb 1986). The differential scaling observed in these osteological structures may affect the direction and force of muscular contraction (e.g., Larson 2005). Further examination of developmental, functional, and biomechanical factors along with interspecific comparisons will be needed to provide more information about the variables shaping anuran skulls during postmetamorphic growth and to interpret the causes of morphological disparity.

Acknowledgments We are deeply indebted to Dr. M. Fabrezi, Dr. L. Trueb, Dr. W. R. Heyer, and anonymous reviewers for their help in improving earlier versions of our work. For loan of specimens employed in this study, we thank S. Kretzschmar and M. Cánepa (Fundación Miguel Lillo), W. R. Heyer (Smithsonian Institution), and H. Zaher (Museu de Zoologia Universidade de São Paulo). This research was supported by the following funds: PIP 112-200801-00225 and PIP 1112008010 402 2422 (CONICET), CIUNT-G430 (UNT), and PICT 2008 578 (FONCYT).

References

Adams DC, Nistri A (2010) Ontogenetic convergence and evolution of foot morphology in European cave salamanders (Family: Plethodontidae). BMC Evol Biol 10:216

Alberch P, Alberch J (1981) Heterochronic mechanisms of morphological diversification and evolutionary change in the Neotropical salamander, *Bolitoglossa occidentalis* (Amphibia: Plethodontidae). J Morphol 167:249–264

Alberch P, Gould SJ, Oster GF, Wake DB (1979) Size and shape in ontogeny and phylogeny. Paleobiology 5:296–317

Bookstein FL (1991) Morphometric tools for landmark data: geometry and biology. Cambridge University Press, Cambridge

Cardini A, Elton S (2007) Sample size and sampling error in geometric morphometric studies of size and shape. Zoomorphology 126:121–134

Ciampaglio CN (2002) Determining the role that ecological and developmental constraints play in controlling disparity: examples from the crinoid and blastozoan fossil record. Evol Dev 4:170–188

Clarke BT (1996) Small size in amphibians: its ecological and evolutionary implications. Symp Zool Soc London 69:201–224

Djorović A, Kalezić ML (2000) Paedogenesis in European newts (*Triturus*: Salamandridae): cranial morphology during ontogeny. J Morphol 243:127–139

Drake AG, Klingenberg CP (2008) The pace of morphological change: historical transformation of skull shape in St Bernard dogs. Proc R Soc B 275:71–76

Duellman WE, Trueb L (1986) Biology of amphibians. The John Hopkins University Press, Baltimore, MD

Dzukic G, Kalezic ML, Tvrtkovic N, Djorovic A (1990) An overview of the occurrence of paedomorphosis in Yugoslav newt (*Triturus*, Salamandridae) populations. Br Herpetol Soc Bull 34:16–22

Eble EJ (2003) Developmental morphospaces and evolution. In: Crutchfield JP, Schuster P (eds) Evolutionary dynamics. Oxford University Press, Oxford, pp 35–65

Emerson SB, Bramble DM (1993) Scaling, allometry, and skull design. In: Hanken J, Hall BK (eds) The skull, vol 3., Functional and evolutionary mechanisms. University of Chicago Press, Chicago, IL, pp 384–421

Fink WL (1982) The conceptual relationship between ontogeny and phylogeny. Paleobiology 8:254–264

Fink WL (1988) Phylogenetic analysis and the detection of ontogenetic patterns. In: McKinney ML (ed) Heterochrony in evolution: a multidisciplinary approach. Plenum, New York, NY, pp 71–91

Frédérich B, Sheets HD (2010) Evolution of ontogenetic allometry shaping giant species: a case study from the damselfish genus *Dascyllus* (Pomacentridae). Biol J Linn Soc 99:99–117

Frédérich B, Vandewalle P (2011) Bipartite life cycle of coral reef fishes promotes increasing shape disparity of the head skeleton during ontogeny: an example from damselfishes (Pomacentridae). BMC Evol Biol 11:82

Frost DR (2011) Amphibian species of the world: an online reference. Version 5.5 (31 January, 2011). Electronic Database accessible at http://research.amnh.org/vz/herpetology/amphibia/. American Museum of Natural History, New York, NY

Gerber S, Neige P, Gunther JE (2007) Combining ontogenetic and evolutionary scales of morphological disparity: a study of early Jurassic ammonites. Evol Dev 9:472–482

Gerber S, Gunther JE, Neige P (2008) Allometric space and allometric disparity: a developmental perspective in the macroevolutionary analysis of morphological disparity. Evolution 62:1450–1457

Gosner KL (1960) A simplified table for staging anurans embryos and larvae with notes on identification. Herpetologica 16:183–190

Goswami A, Prochel J (2007) Ontogenetic morphology and allometry of the cranium in the common european mole (*Talpa europaea*). J Mamm 88:667–677

Gould SJ (1966) Allometry and size in ontogeny and phylogeny. Biol Rev 41:587–640

Gould SJ (1977) Ontogeny and phylogeny. Harvard University Press, Cambridge

Hanken J (1984) Miniaturization and its effects on cranial morphology in plethodontid salamanders, genus *Thorius* (Amphibia: Plethodontidae). I. Osteological variation. Biol J Linn Soc 23:55–75

Hanken J, Wake DB (1993) Miniaturization of body size: organismal consequences and evolutionary significance. Annu Rev Ecol Syst 24:501–519

Heyer WR (1969) Studies on the genus *Leptodactylus* (Amphibia, Leptodactylidae) III. A redefinition of the genus *Leptodactylus* and a description of a new genus of Leptodactylid frogs. Contrib Sci Nat Hist Mus Los Angel Cty 155:1–14

Heyer WR (1978) Systematics of the *fuscus* group of the genus *Leptodactylus* (Amphibia, Leptodactylidae). Contrib Sci Nat Hist Mus Los Angel Cty 29:1–85

Heyer RW (2005) Variation and taxonomic clarification of the large species of the *Leptodactylus pentadactylus* species group (Amphibia: Leptodactylidae) from Middle America, Northern South America, and Amazonia. Arq Zool 37:1–86

Heyer RW, Juncá FA (2003) *Leptodactylus caatingae*, a new species of frog from eastern Brazil (Amphibia: Anura: Leptodactylidae). Proc Biol Soc Wash 116:317–329

Heyer WR, García-Lopez JM, Cardoso A (1996) Advertisement call variation in the *Leptodactylus mystaceus* species complex (Amphibia: Leptodactylidae) with a description of a new sibling species. Amphib–Reptil 17:7–31

Holm S (1979) A simple sequential rejective multiple test procedure. Scand J Stat 6:65–70

Hone DWE, Dyke GJ, Haden M, Benton MJ (2008) Body size evolution in Mesozoic birds. J Evol Biol 21:618–624

Ivanović A, Vukov T, Džukic G, Tomašević N, Kalesić ML (2007) Ontogeny of skull size and shape changes within a framework of

biphasic lifestyle: a case study in six *Triturus* species (Amphibia, Salamandridae). Zoomorphology 126:173–183
Klingenberg CP (1998) Heterochrony and allometry: the analysis of evolutionary change in ontogeny. Biol Rev 73:79–123
Klingenberg CP (2010) Evolution and development of shape: integrating quantitative approaches. Nature 11:623–634
Klingenberg CP (2011) MORPHOJ: an integrated software package for geometric morphometrics. Mol Ecol Resour 11:353–357
Klingenberg CP, McIntyre GS (1998) Geometric morphometrics of developmental instability: analyzing patterns of fluctuating asymmetry with Procrustes methods. Evolution 52:1363–1375
Klingenberg CP, Duttke S, Whelan S, Kim M (2011) Developmental plasticity, morphological variation and evolvability: a multilevel analysis of morphometric integration in the shape of compound leaves. J Evol Biol 25:115–129
Larson PM (2002) Chondrocranial development in larval *Rana sylvatica* (Anura: Ranidae): a morphometric analysis of cranial allometry and ontogenetic shape change. J Morphol 252:131–144
Larson PM (2004) Chondrocranial morphology and ontogenetic allometry in larval *Bufo americanus* (Anura, Bufonidae). Zoomorphology 123:95–106
Larson PM (2005) Ontogeny, phylogeny, and morphology in anuran larvae: morphometric analysis of cranial development and evolution in *Rana* tadpoles (Anura: Ranidae). J Morphol 264:34–52
McNamara KJ (1986) A guide to the nomenclature of heterochrony. J Paleontol 60:4–13
Mitteroecker P, Gunz P, Bookstein FL (2005) Heterochrony and geometric morphometrics: a comparison of cranial growth in *Pan paniscus* versus *Pan troglodytes*. Evol Dev 7:244–258
Ponssa ML (2008) Cladistic analysis and osteological descriptions of the species of the *L. fuscus* species group of the genus *Leptodactylus* (Anura, Leptodactylidae). J Zool Syst Evol Res 46:249–266
Ponssa ML, Jowers MJ, De Sá RO (2010) Osteology, natural history notes, and phylogenetic relationships of the poorly known Caribbean frog *Leptodactylus nesiotus* (Anura, Leptodactylidae). Zootaxa 2646:1–25
Reilly SM, Wiley EO, Meinhardt DJ (1997) An integrative approach to heterochrony: the distinction between interspecific and intraspecific phenomena. Biol J Linn Soc 60:119–143
Rohlf J (2010a) TpsDig program version 1.49. Ecology and evolution, SUNY at Stony Brook
Rohlf J (2010b) TpsRelw program version 2.16. Ecology and evolution, SUNY at Stony Brook
Rohlf FJ, Bookstein FL (1990) Proceedings of the Michigan Morphometrics Workshop. Special publication no. 2. University of Michigan Museum of Zoology, Ann Arbor, MI
Shea BT (1983) Allometry and heterochrony in the African apes. Am J Phys Anthropol 62:275–289
Shea BT (1985) Ontogenetic allometry and scaling: a discussion based on the growth and form of the skull in African apes. In: Jungers WL (ed) Size and scaling in primate biology. Plenum Press, New York, NY, pp 175–205
Sheets H (2004) Morphometrics software: IMP-Integrated morphometrics package. http://www.canisius.edu/~sheets/morphsoft.html
Stanley SM (1973) An explanation for Cope's Rule. Evolution 27:1–26
Viscosi V, Cardini A (2011) Leaf morphology, taxonomy and geometric morphometrics: a simplified protocol for beginners. PLoS One 6:1–19
Wake MH (1986) The morphology of *Idiocranium russeli* (Amphibia: Gymnophiona), with comments on miniaturization through heterochrony. J Morphol 189:1–16
Wassersug RJ (1976) A procedure for differential staining of cartilage and bone in hole formalin fixed vertebrates. Stain Technol 51:131–134
Webster M, Zelditch ML (2005) Evolutionary modifications of ontogeny: heterochrony and beyond. Paleobiology 31:354–372
Wilson LA, Sánchez-Villagra MR (2010) Diversity trends and their ontogenetic basis: an exploration of allometric disparity in rodents. Proc R Soc B 277:1227–1234
Yeh J (2002) The effect of miniaturized body size on skeletal morphology in frogs. Evolution 56:628–641
Zelditch ML, Sheets HD, Fink WL (2000) Spatio-temporal reorganization of growth rates in the evolution of ontogeny. Evolution 54:1363–1371
Zelditch ML, Sheets HD, Fink WL (2003) The ontogenetic dynamics of shape disparity. Paleobiology 29:139–156
Zelditch ML, Swiderski HD Sheets, Fink WL (2004) Geometric morphometrics for biologists: a primer. Elsevier Academic Press, New York, NY